High Power ECR Ion Thruster Discharge Characterization

IEPC-2005-272

Presented at the 29th Electric Propulsion Conference, Princeton University,

October 31 – November 4, 2005

John E. Foster[†], Hani Kamhawi[‡], Tom Haag[§], Christian Carpenter[**], and George Williams[††].

NASA Glenn Research Center, Cleveland, OH, 44135

Abstract: Electron cyclotron resonance (ECR) based ion thrusters with carbon based ion optics can potentially satisfy lifetime requirements for long duration missions (~10 years) because grid erosion and cathode insert depletion issues are virtually eliminated. Though the ECR plasma discharge has been found to typically operate at slightly higher discharge losses than conventional DC ion thrusters (for high total thruster power applications), the discharge power fraction is small (less than 1 percent at 25 kW). In this regard, the benefits of increased life, low discharge plasma potentials, and reduced complexity are welcome tradeoffs for the associated discharge efficiency decrease. Presented here are results from discharge characterization of a large area ECR plasma source for gridded ion thruster applications. These measurements included load matching efficacy, bulk plasma properties via Langmuir probe, and plasma uniformity as measured using current probes distributed at the exit plane. A high degree of plasma uniformity was observed (flatness >0.9). Additionally, charge state composition was qualitatively evaluated using emission spectroscopy. Plasma induced emission was dominated by xenon ion lines. No doubly charged xenon ions were detected.

Introduction

The High Power Electric Propulsion (HiPEP) thruster was designed and built to address the need for a long life, high specific impulse option to satisfy requirements for missions to the outer planets and the outer edge of the solar system as was originally identified by NASA.[1,2] These powerful thrusters would utilize a nuclear reactor source to provide the necessary electrical energy. For such missions, ion thrusters may be required to operate for up to 10 years.[2] Because of the unprecedented long lifetimes required, innovative solutions to grid and cathode life were pursued in the development of this device. High specific impulse operation requires high beam voltages and correspondingly a more negative accelerator voltage. Associated with a more negative accelerator grid is increased charge exchange erosion which can lead to thruster failure. Carbon-based ion optics which are more resistant to sputter erosion at energies of interest than ordinary metal grids were pursued as the solution to grid erosion.[1,23] Indeed, graphite was has a sputter yield that is nearly 10 times lower than that of molybdenum, the primary material for present-day ion thrusters. To minimize grid wear, in addition to fabricating the grids from graphite, the size of the HiPEP thruster was selected such that operating current density was slightly less than 1 mA/cm^2. The selected geometrical shape of the optics and the discharge chamber was rectangular. This shape allows for straightforward

[†] Aerospace Engineer, The Electric Propulsion Branch, John.E.Foster@NASA.gov.
[‡] Aerospace Engineer, The Electric Propulsion Branch, Hani.Kamhawi@NASA.gov
[§] Aerospace Engineer, The Electric Propulsion Branch, Thomas.Haag@NASA.gov
[**] Aerospace Engineer, The Electric Propulsion Branch, Formerly QSS, christian.carpenter@rocket.com.
[††] Aerospace Engineer, The Electric Propulsion Branch, George.W.Williams@ grc. NASA.gov

scaling to higher power levels with minimal modifications to the magnetic circuit such as simple lateral stretching of the discharge chamber. This rather straightforward modification allows for the thruster size to change in accordance with changes in mission requirements.

Due to exposure to ion bombardment from both ambient discharge plasma ions and locally produced energetic ions and to the depletion of the work function impregnate material over time, hollow cathode operational lifetime is also inherently limited.[4,5,6] The longest documented operating time for a hollow cathode in an ion thruster is ~30 kHrs.[7] Thruster operating times for missions being planned to the outer planets are well in excess of this state of the art lifetime. Several novel solutions to the cathode lifetime problem has been proposed. These include: 1) microwave electron cyclotron resonance (ECR) plasma production[1] 2) multiple cathode operation[8], 3)reservoir cathode[9], and 4) high current conventional cathode[10]. The work presented herein focuses on the microwave electron cyclotron resonance plasma production effort. By electrodelessly producing the plasma, lifetime issues associated with hollow cathode operation are virtually eliminated. ECR discharges offer many distinct advantages over DC cathodes:[1,11,12,13]

- Microwave discharge plasma production lifetime is limited only by the life of the power tube.
- Microwave power tubes have demonstrated on-orbit lifetimes in excess of 10 yrs.
- A single microwave power tube can supply power to both the main discharge and the neutralizer.
- The ECR discharge eliminates the need for separate cathode and main flow injection systems, which should result in propellant savings and reduced feed system complexity.
- Expensive, high purity xenon gas purity is not a requirement; Low purity xenon can be used in a microwave thruster thereby yielding considerable cost savings.
- ECR discharges operate at reduced plasma potentials which translate into reduced sputter erosion of the upstream surface of the screen grid electrode.
- System complexity is significantly reduced.
- Microwave power generation tubes are fairly efficient with magnetrons having electrical efficiencies as high as 90%.
- The microwave power tubes and associated power electronics masses are comparable to that of conventional DC Power Processing Unit (PPU) electronics.
- Additional mass savings can be realized through the use of the very lightweight, copper coated graphite waveguide components.
- Because the main discharge cathode is eliminated, heavy, high current lines are eliminated.
- Physical wires, whose insulation is susceptible to radiation damage, are eliminated for the main discharge and neutralizer components.

The use of electrodeless discharges for plasma production has long been identified as a means to resolve lifetime issues. Serious investigations of microwave-based ion thrusters at NASA Glenn dates back to the 1980s. Here discharge-only testing was utilized as a means of assessing the suitability of this technology to ion thrusters.[14] The Japanese space agency has maintained a vigorous microwave ion thruster research and development effort dating from the late 1980s to the present. This work culminated in the launch of a space science mission to an asteroid using ECR ion thrusters.[15] A revival in microwave research began at NASA GRC in 2002. This work culimated in the testing and eventual beam extraction from a 40 cm ion source. The focus of this effort was to develop a medium power thruster similar to the NEXT engine. Discharge characterization results from that study were promising.[16] Leveraging the findings from the 40 cm microwave thruster effort, a rectangular microwave ion source was proposed and pursued under the HIPEP project. This work culminated with the operation of the largest (dimensionally) and highest power microwave ion thruster ever tested: 15 kW. This engine operated at 2.45 GHz. Part of the development effort under the HiPEP project was to understand operation at the original operating frequency of 2.45 GHz and then move to a higher frequency of 5.85 GHz. Calculations indicated that operating the engine at 5.85 GHz not only satisfied performance requirements but it also allowed for growth to higher beam currents to accommodate performance requirement changes as dictated by the mission. The following is discussed: 1) design considerations for the microwave ion source are discussed in light of performance and mission implications 2) the experimental setup is commented upon, and finally 3) a discussion of the characterization of discharge operation utilizing electrostatic probes and emission spectra is presented. It should be pointed out that the microwave discharge characterized and studied in this effort is designated a high power (700W to 2500 W) plasma source in contrast to low power sources studied and developed at JAXA/ISAS for the MUSES C (<35 W) mission

and medium discharge power sources (100 W-300 W) also studied at NASA GRC.[16] It should be also pointed out that microwave neutralizer development is not covered in this work. A summary of these efforts may be found elsewhere.[13,17,18]

Basic Design and Discharge Performance Implications

A. Plasma Discharge Requirements

An ion thruster discharge plasma must be capable of supplying enough ions per unit time to satisfy the beam extraction current requirement. In this regard, for a given beam current, a minimum plasma density is necessary to supply sufficient thermal ion flux to the ion extraction surface. Conventional ion thrusters utilize produce the discharge plasma by injecting electrons from a hollow cathode into the discharge chamber. These electrons bombard the neutral gas also injected into the discharge chamber to produce the plasma. The presence of a multi-pole magnetic circuit increases the containment length of injected primary electrons thereby improving discharge efficiency. Figure 1 illustrates the variations in the ion current available for extraction as a function of plasma density at three different electron temperatures for the HiPEP rectangular ion source. The electron temperatures selected here are typical of ion thruster operation.[16,19,20] For these calculations, the extraction plane is 40 cm by 90 cm with an the effective screen grid transparency set at 80%.

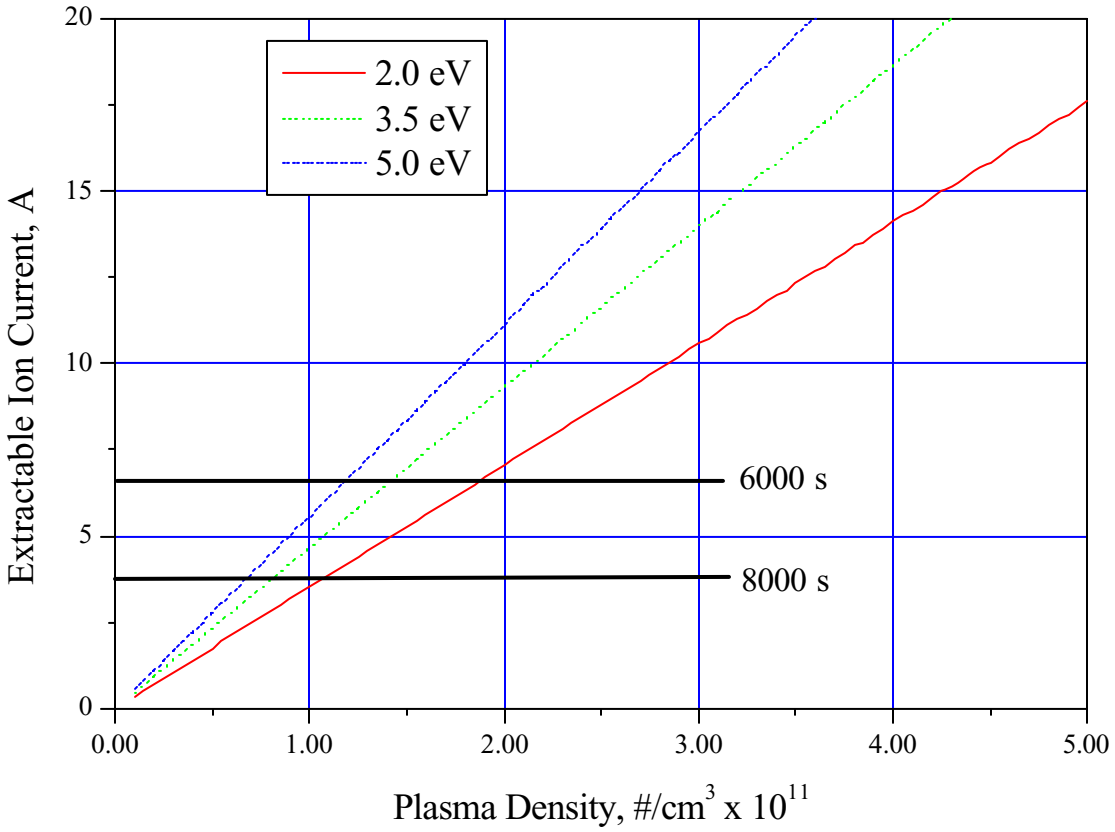

Figure 1. Extractable ion current as a function of plasma density and electron temperature.

To meet beam current performance targets over the 6000 s to 8000 s range (25 kW HiPEP), the plasma density near the ion optics must be sufficiently high as indicated in the figure.

In addition to meeting the beam current magnitude requirement, the discharge plasma should also be uniform. High uniformity leads to:

- Simplified ion optics design
- Minimal localized wear
- Reduced thermal loads
- Increased total thruster efficiency
- A uniform backstreaming limit independent of aperture location

Because of the central location of the hollow cathode, extremely flat density profiles across the diameter of the device are in practice difficult to achieve in conventional DC ion thrusters. This is primarily due to the high degree of ionization that takes place on axis, which tends to give rise to a peaked plasma density profile.[21]

Another important attribute of a discharge plasma is plasma potential. In particular, the potential difference between the local plasma potential and the screen potential. Because the energy of ions flowing to the screen grid is determined by this potential difference, low discharge plasma potentials minimize the impact energy and thus erosion of screen grid. It should also be pointed out that the discharge plasma must be stable and thus free from voltage and current oscillations

In contrast to conventional DC ion thrusters, microwave plasma sources heat electrons in ECR zones to ionization energies. In this regard, the ECR plasma production sites generate the discharge plasma. These sites also load the magnetic field with hot electrons, which generates secondary plasma not unlike a DC multipole source. Typical plasma densities generated in such discharges range between 10^{11} -10^{12} #/cm^3 at low microwave frequencies (< 6 GHz). If over-dense plasma production is neglected, then the microwave excitation frequency determines to first order the maximum discharge plasma density attainable in the ion source. Typically, these maximum plasma densities are achieved only at the ECR heating sites. Usually, bulk plasma densities are somewhat less than this maximum value. The maximum density refers to the magnitude of plasma density of which the microwave radiation no longer propagates but is reflected instead. In this case, the microwaves can penetrate only by tunneling with a penetration depth of order the wavelength. Operation at higher microwave frequencies allows higher plasma densities to be achieved before reaching the critical "cut-off" plasma density. The maximum plasma density obtainable can be calculated to first order from relatively simple relations. Electron cyclotron resonance takes place at regions of where the microwave frequency equals the electron gyro-frequency. The plasma in the ECR zones can reach a maximum density determined by the cut-off condition where the microwave frequency equals the local plasma frequency. The plasma frequency and cyclotron frequency are defined below:

$$\omega_p = \sqrt{\frac{n \cdot e^2}{m_e \cdot \varepsilon_o}} \qquad (1)$$

and

$$\omega_{ce} = \frac{B \cdot e}{m_e} \qquad (2)$$

Here, B is the magnetic field, e is elementary charge on the electron, m_e is the mass of the electron, n is the plasma density, and ε_o is the permittivity of free space. At plasma densities higher than the criterion established by the condition, $\omega_{ce} = \omega_p$, the microwaves are no longer absorbed, but reflected to regions of lower field strength.

The density limitations experienced by microwave certain ECR engine designs can be circumvented by means other than increasing the operating frequency. These approaches, of course, can be used to a certain degree in conjunction with frequency increases as well. These approaches include:

- Altering the magnetic circuit near the microwave applicator
- Changing the way in which the microwaves are launched.

These additional approaches are typically necessary because arbitrarily increasing the microwave frequency is not practical. Arbitrary increases in the frequency require higher magnetic fields to establish ECR zones. These high magnetic fields make it difficult for plasma to diffuse away from ECR plasma production zones. Additionally, ECR zones occur much closer to the magnet surface which gives rise to increases in plasma losses to the walls. In this respect, arbitrarily increasing the microwave frequency is not necessarily the most effective or practical means to increase performance.

The initial microwave operation of the HiPEP thruster was at 2.45 GHz. The microwaves were injected using a slotted antenna[22] and permanent magnetic circuit to: a) establish ECR production zones and b) to provide for electron confinement. Figure 2 illustrates variations in plasma density at cut-off with microwave frequency. Also shown in the figure is the variation in required magnetic field strength with frequency. High-energy product samarium cobalt magnets are capable of generating up to 2.8 kG near the magnets surface. This puts the practical limit on the operating frequency of around 6 GHz. The second generation HiPEP engine utilized 5.85 GHz microwave radiation to generate the discharge plasma. The arrow in the figure indicates the required field strength and plasma density at cutoff at this frequency. It should be pointed at this operating frequency, the HiPEP engine satisfies the beam current requirements at the operating design points with substantial margin (>2x), provided the bulk density also approaches this value.

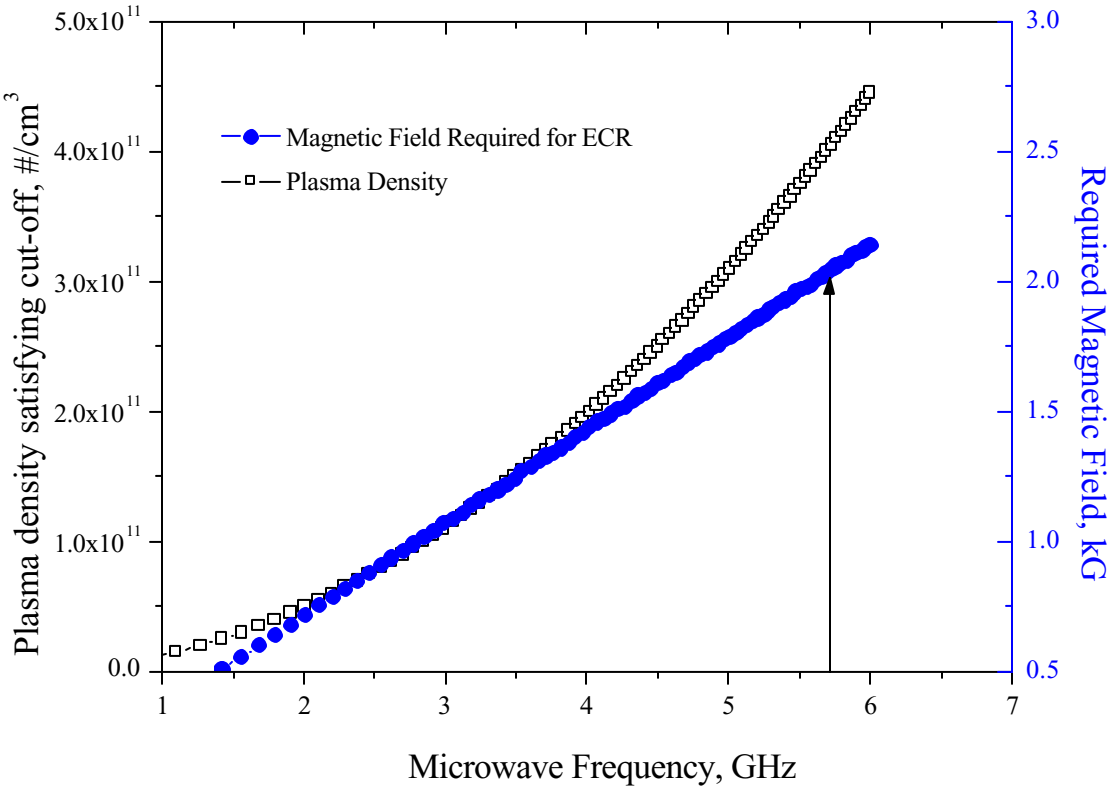

Figure 2. Calculated variations in maximum plasma density with microwave frequency.

B. Discharge Performance Implications

A design parameter that characterizes the efficiency of plasma production is the discharge losses. Simply put, it is the ratio of discharge power to ion current extracted. In this respect, it is somewhat sensitive to grid geometry (physical transparency). The traditional objective of ion source design is to minimize this parameter. For low to medium power ion thrusters, the discharge losses can constitute a significant fraction of the input power. However, for high power systems such as HIPEP, typically, the discharge power accounts for less than a few percent of the total thruster power. In general, DC based ion sources are more efficient than microwave sources. This stems primarily from the fact that in a DC system, electrons are injected via hot cathode into the discharge to ionize the gas. This is in contrast to microwave based systems where the electrons must be first produced by break down of the gas and then subsequently heated via ECR. But because discharge losses account for such a small fraction of the total input power for high power systems, the trade of extended lifetime for discharge efficiency obtained when using an electrodeless plasma production scheme such as ECR is an acceptable approach.

Figure 3 illustrates the sensitivity of efficiency and thrusting time to discharge losses for a 25 kW ion thruster system.[23] DC ion sources operate between 150 and 200 W/A at discharge utilizations around 90%.[24] Discharge losses in the microwave HiPEP thruster appear to be roughly twice that of a DC thruster. Even so, a microwave system with such discharge losses can nearly match a 200 W/A source provided it can operate at high discharge propellant utilization efficiencies. Usually, this is possible with microwave thrusters because of associated low plasma potentials. In contrast, high propellant utilization operation in DC ion thrusters is undesirable due to the higher discharge plasma potentials and the increased doubly charged xenon to singly charged xenon ratios, both of which increase cathode and screen grid erosion rates. For a Jupiter Grand Tour-type mission, trip times for a thruster with higher discharge losses (500 W/A, for example) are also comparable to 200 W/A DC thruster provided it can operate at sufficiently high discharge utilizations. A microwave system with 500W/A and 95 % discharge utilization yields trip times comparable to a 200 W/A DC system operating at 90% propellant utilization.

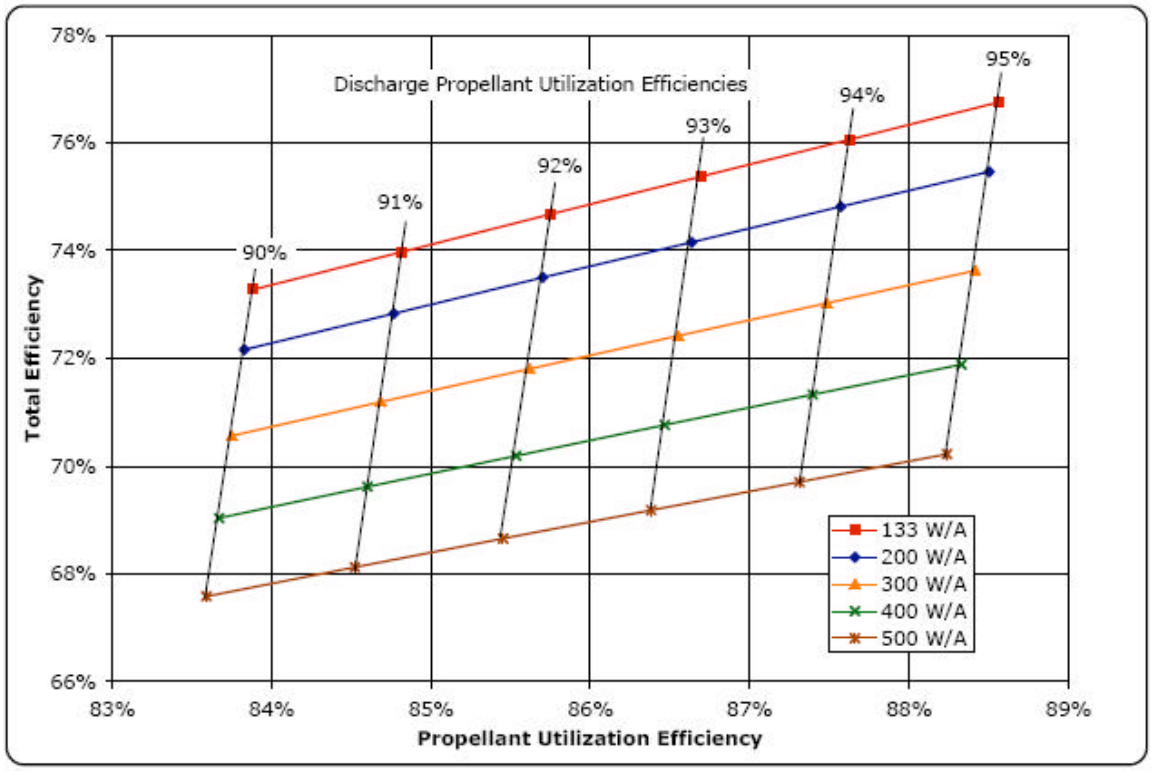

Figure 3a. Sensitivity of total efficiency to discharge losses.[23]

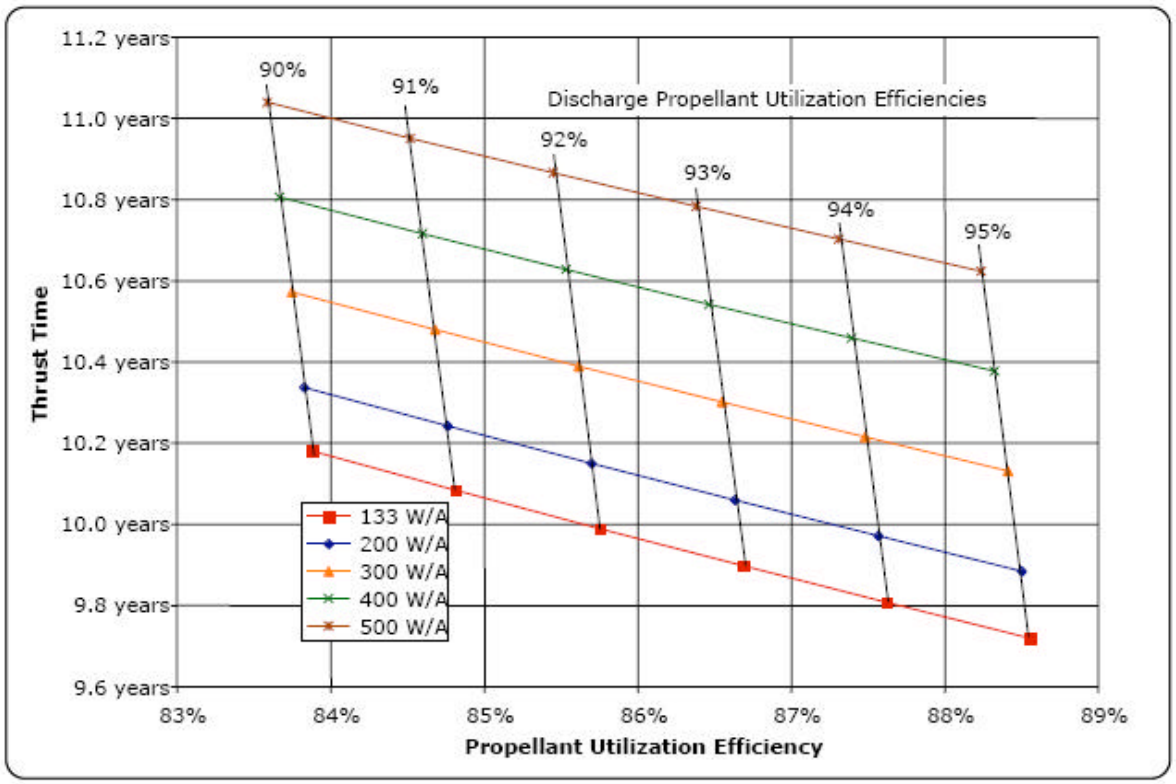

Figure 3 b. Sensitivity of thrust time to discharge losses.[23]

Early Microwave Ion Source Development

A. Discharge Testing

As mentioned earlier, at the inception of the experimental phase of the HiPEP project, a microwave ion source was fabricated. This first generation source operated at 2.45 GHz. The ion source also utilized a slotted antenna design. The discharge itself demonstrated operation over a wide background pressure range extending from 1×10^{-6} Torr up to 100 mTorr. Discharge characterization was done on this source to determine general source operation characteristics as well as determine the range of extractable ion current as a function of microwave power. Figure 4 demonstrates the change in ion current collected at the grid as a function of microwave power (2.45 GHz) as acquired in Vacuum Facility 11 (2.2 m diameter, 7.9 m long) The xenon flow rate was set at 42 SCCM. The ion current increased linearly with increasing input microwave power. Assuming 95% discharge utilization, the maximum ion current available would be only 2.9 A. To achieve 2.9 A of ion current according to the slope indicated by Figure 4, the discharge would have to operate around 1750 W. Because discharge losses during discharge-only operation tend to be lower than those assessed during beam extraction conditions, it is expected that the required power to extract the 2.9 A would be somewhat larger than this. The need to achieve a higher beam current at a lower discharge power was another driver to investigating operation at the higher microwave frequencies. Langmuir probe data as well as emission spectra were acquired during discharge characterization as well. It was found at the 750 W input power condition, as measured near the ion grid, the electron temperature was approximately 3 eV with plasma potentials around 10 V. The plasma density at this power level was as high as 6×10^{10} #/cm^3, very close to the cutoff density at this frequency.

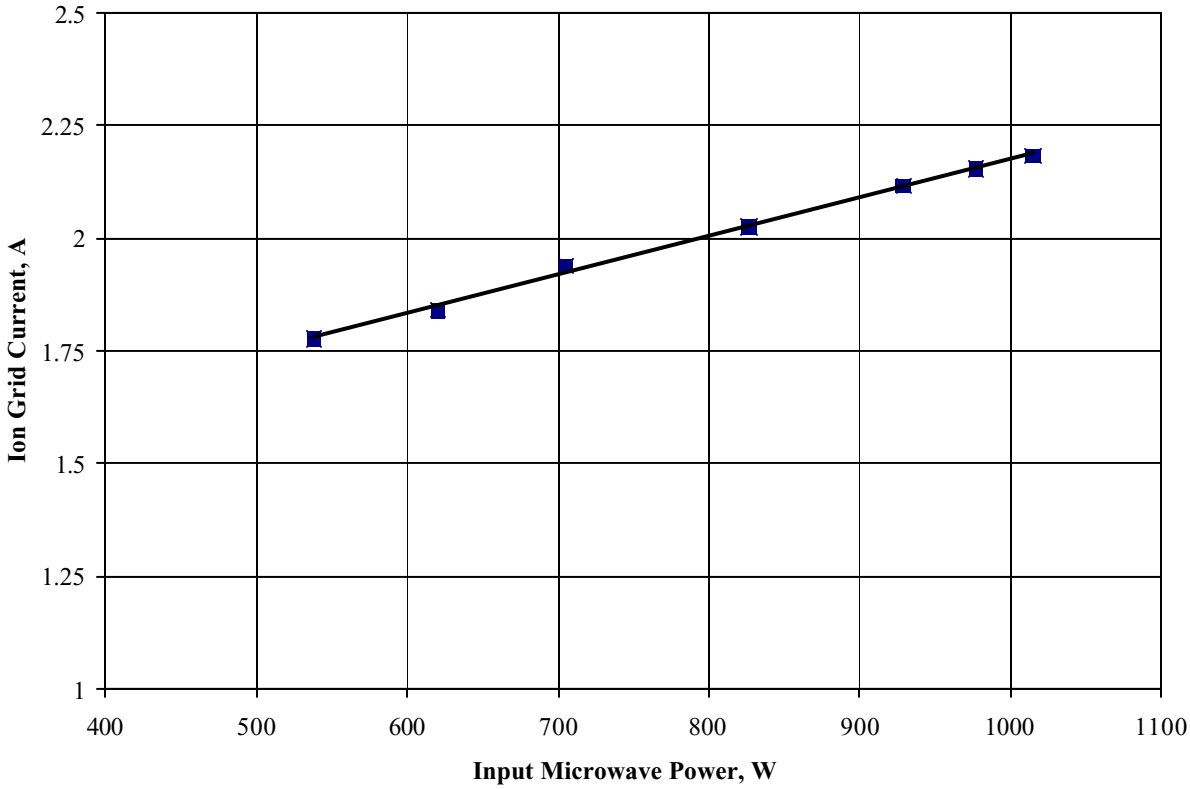

Figure 4. Variation in collected ion grid current with increasing microwave power.

The 2.45 GHz discharge testing culminated in a full scale beam extraction test. A simplified schematic of the extraction test is indicated in Figure 5a. A DC block was used to isolate the thruster from ground while at the same time allow for the transport of microwaves to the engine. A view of discharge only operation as well as one depicting beam extraction is shown in Figure 5b.

During the beam extraction tests, thruster power was varied from 6 kW up to 16 kW, well over half the target operating power level of 25 kW. Discharge only testing indicated that the plasma profile was fairly uniform. This assessment was inferred from ion collecting probes mounted to the ion grid. Figure 5c depicts a lateral sweep of a Faraday probe across the middle of the plume during beam extraction. The flatness of the beam profile suggests that indeed the plasma is reasonably uniform at least across the middle of the thruster. The data presented here corresponds to a 1.33 A beam at 6500 V beam voltage. Absent was the centerline peak typically observed in DC ion thruster due to the on axis cathode which invariably gives rise to poorer beam flatness. All in all, data taken at 2.45 GHz was certainly promising but it did point to the need for operation at a higher frequency to increase plasma density and propellant utilization. Additionally, the test represented the largest, highest powered microwave ion thruster ever operated.

After the beam extraction test at 2.45 GHz, the microwave thruster effort turned toward implementing 5.85 GHz operation. The slotted antenna approach was used in this case as well. The primary change to the thruster hardware was a relatively straightforward resizing of the antenna waveguide and associated slots. Preliminary testing of this device was also quite promising. Figure 5d presents a plot of ion current collected at a ion optics simulator grid as a function of microwave power and flow rate. The current collected here represents an upper limit of the maximum extractable ion current. As can be seen here, collected ion grid currents are well within the required range for effective thruster operation.

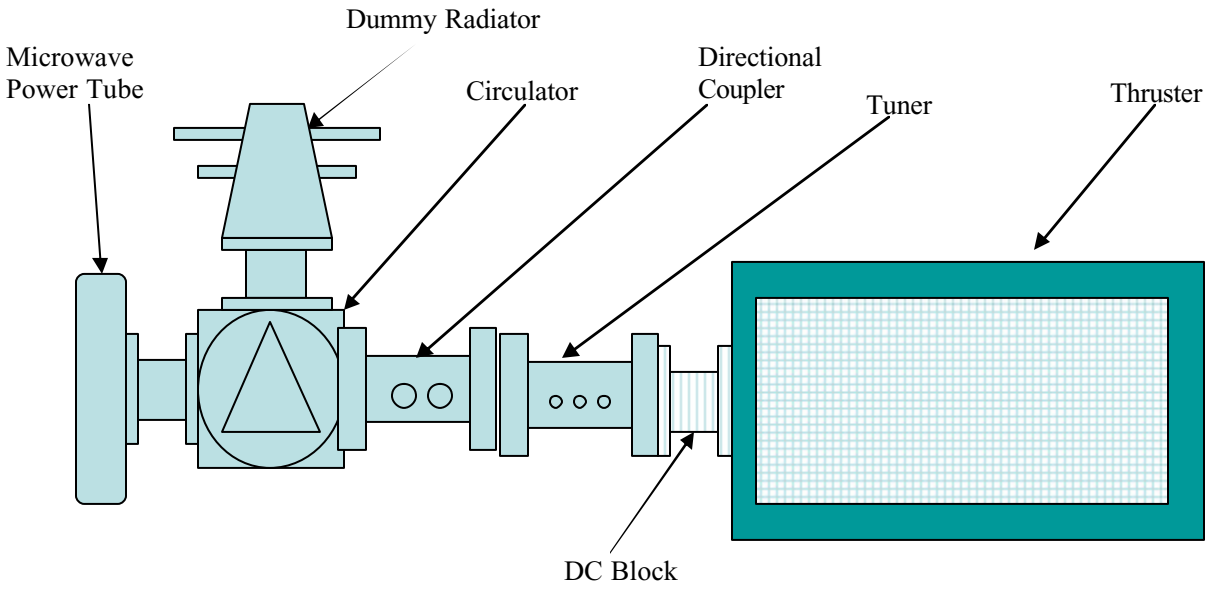

Figure 5a. Experimental set-up for beam extraction at 2.45 Ghz. Note presence of the DC block.

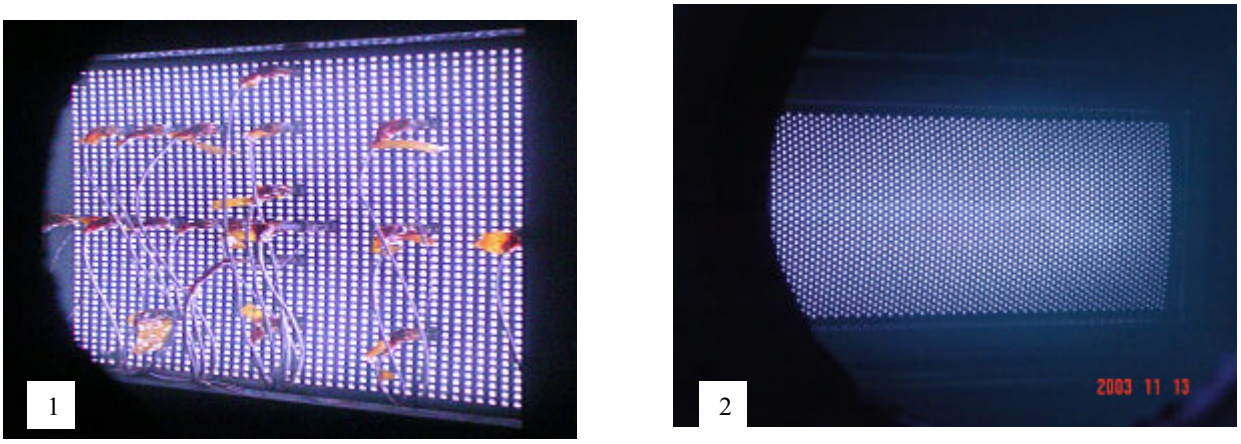

Figure 5b. 1) Discharge only operation . Note ion grid probes, which were used to measure flatness.
2) Beam extraction: Ion beam =2.2 A; 16kW thruster power.

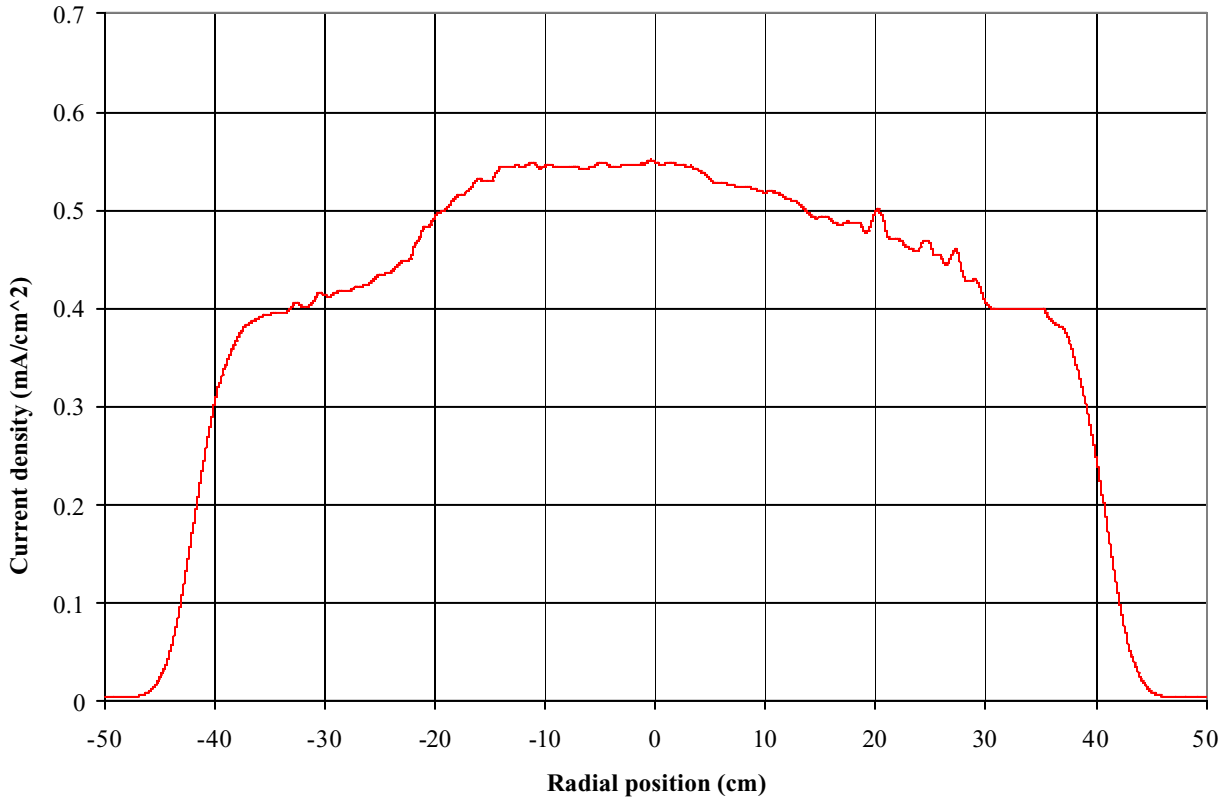

Figure 5c. Centerline current density profile at 0.02 m downstream of optics. Beam voltage: 6500 V, Beam current 1.33 A.

As indicated in the Figure 5d, it was possible to operate the source well over the equivalent Ampere of input xenon flow (3.1 A). This suggests significant re-ingestion of ions that recombine on the collector grid. Continued optimization of the source magnetic circuit improved overall performance. Continued optimization is the focus of existing efforts. The operating characteristics of this evolved source are the subject of this paper and are discussed in detail in the sections that follow.

Test Setup

A. Test facility

The bulk of the discharge testing described herein took place in the NASA GRC Vacuum Facility 2 space simulation chamber. This vacuum facility measures 2.2 m long and 1 m in diameter. The facility is evacuated via a large, 30 cm turbomolecular pump backed by an oil-free roughing pump. The pumping speed is approximately 2000 l/s. Base pressure is approximately 6×10^{-6} Torr. During discharge operation, tank pressure resides in the mid- 10^{-4} Torr range. Due to pumping speed limitations, flow rates above 40 SCCM (~65 percent of full power condition) could not be investigated due to the unacceptably high background pressure. Further characterization of the microwave source at higher flow rates is left to future work. Unless otherwise stated, xenon was the working gas for the tests described herein.

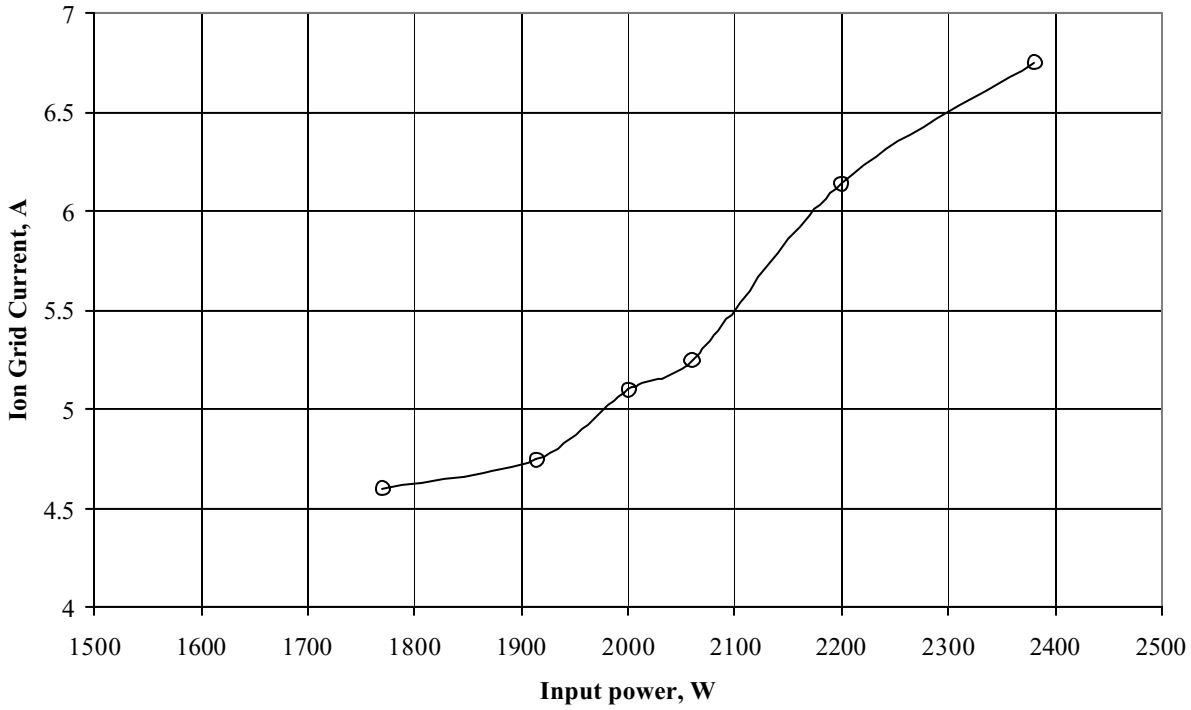

Figure 5d. Variation in collected ion grid current with input microwave power at 38 SCCM.

B. Microwave thruster discharge chamber

With the exception of the magnetic circuit, mechanically the discharge chamber investigated in this work is nearly identical to that of the DC HiPEP thruster discharge chamber, which demonstrates flexibility of design.[1] The magnetic circuit for this work was designed and optimized for microwave ECR plasma production. The microwaves are injected into the chamber via a slotted antenna, a radiating structure commonly used for communication applications. A slotted antenna refers to any waveguide or radiating structure that contains radiating, periodically spaced apertures.[22] The slotted antenna is designed such that the microwave power is distributed evenly to each slot or aperture. A more detailed description of the discharge chamber may be found in reference 1. The ion extraction plane was terminated with a grid simulator. The grid simulator consisted of a stainless steel grid with 1 cm apertures. The open area fraction of the grid was 50%. The grid could be biased to measure ion current flux at the exit plane of the discharge chamber. Affixed to the diagnostic grid but facing upstream were l4 button probes used for plasma diagnostics as will be discussed in the following section. WR 159 waveguide was used to transport the microwaves from a 3 kW, single cavity, klystron amplifier which was excited at 5.85 GHz. The discharge chamber was tested at microwave input powers ranging from 700 W to over 2 kW corresponding to power densities of 0.01 to 0.02 W/cm^3. Owing to the discharge chamber's large size/volume, the microwave power density is an order of magnitude lower than smaller, lower power devices such as the ISAS MUSES C engine.[25] In general, such power densities are too low to generate a discharge plasma throughout the entire volume. In ECR microwave sources most of the power is actually concentrated at the ECR zones. In these bcalized ECR zones, the power densities are substantial. A schematic of the test setup is shown in Figure 6. A high power, 4-port circulator managed reflected power. Reflected power was channeled to high power, convectively cooled dummy loads. A two port bi-directional waveguide coupler connected to power meters was used to estimate the forward and reflected power at the discharge chamber. The net microwave power entering the discharge chamber was consistent with discharge chamber radiated output power as determined using a field meter. A four stub tuner was used for impedance matching. Microwaves

flowed into the chamber via an alumina, microwave window. The microwave window served as a vacuum seal. In most cases, the fraction of reflected power during plasma production was less than 5 percent.

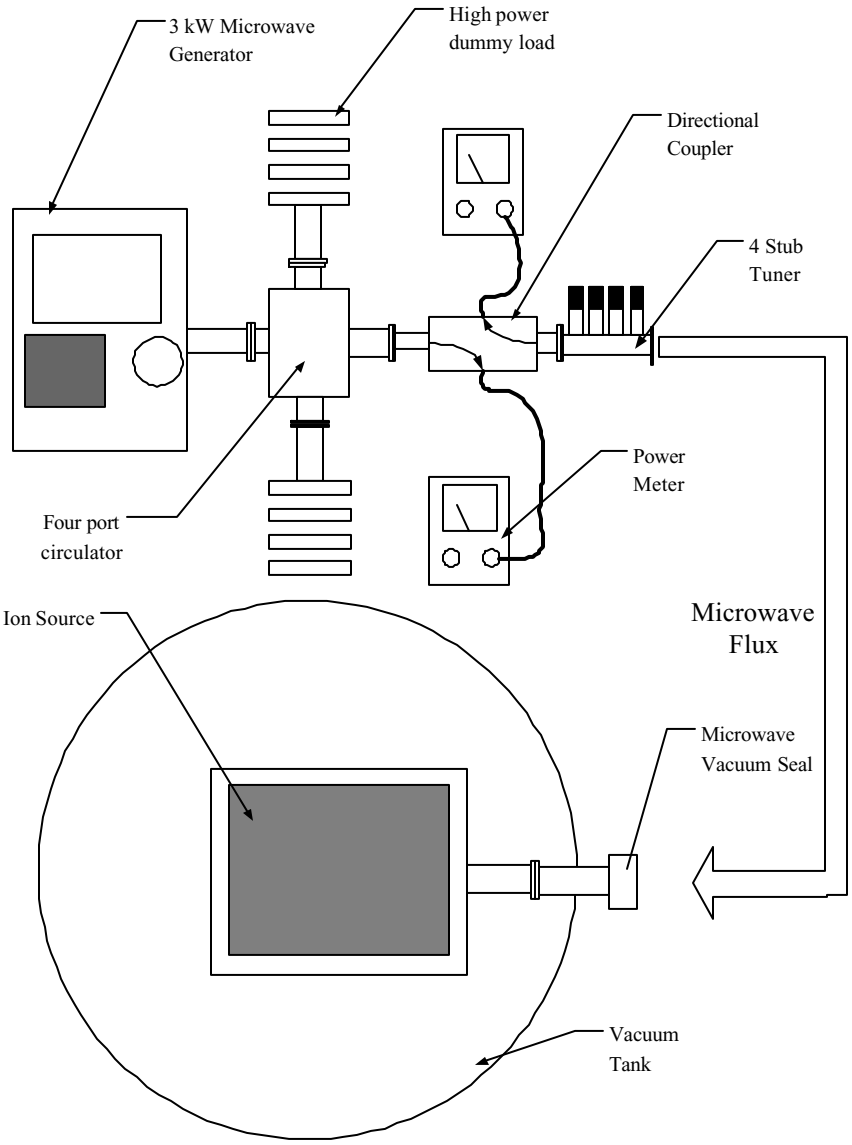

Figure 6. Layout of the test set-up. Arrow indicates the transport of microwave power into the tank.

C. Diagnostics

A number of diagnostics were used to assess the operation of the discharge plasma. The termination grid itself could be biased to extract maximum current flux to the exit plane. In practice, it was found that at collected current levels over 1 A, arcing between the grid and tank resulted. Presumably, the arcing conditions are enhanced due to the relative closeness of the grid to the chamber wall and the increased plasma flux to the walls during operation. Rather than bias the grid, an array of 14 planar probes distributed over the grid surface was used to determine the uniformity and average current density at the exit plane. Each molybdenum probe measured 6.35 mm in diameter. Each probe was housed in a ceramic bushing to isolate it from the ion collector grid. A layout of the probe locations is depicted in Figure 7. The location (0,0) is the center of the discharge chamber. Off-center probes were used to assess discharge transverse symmetry.

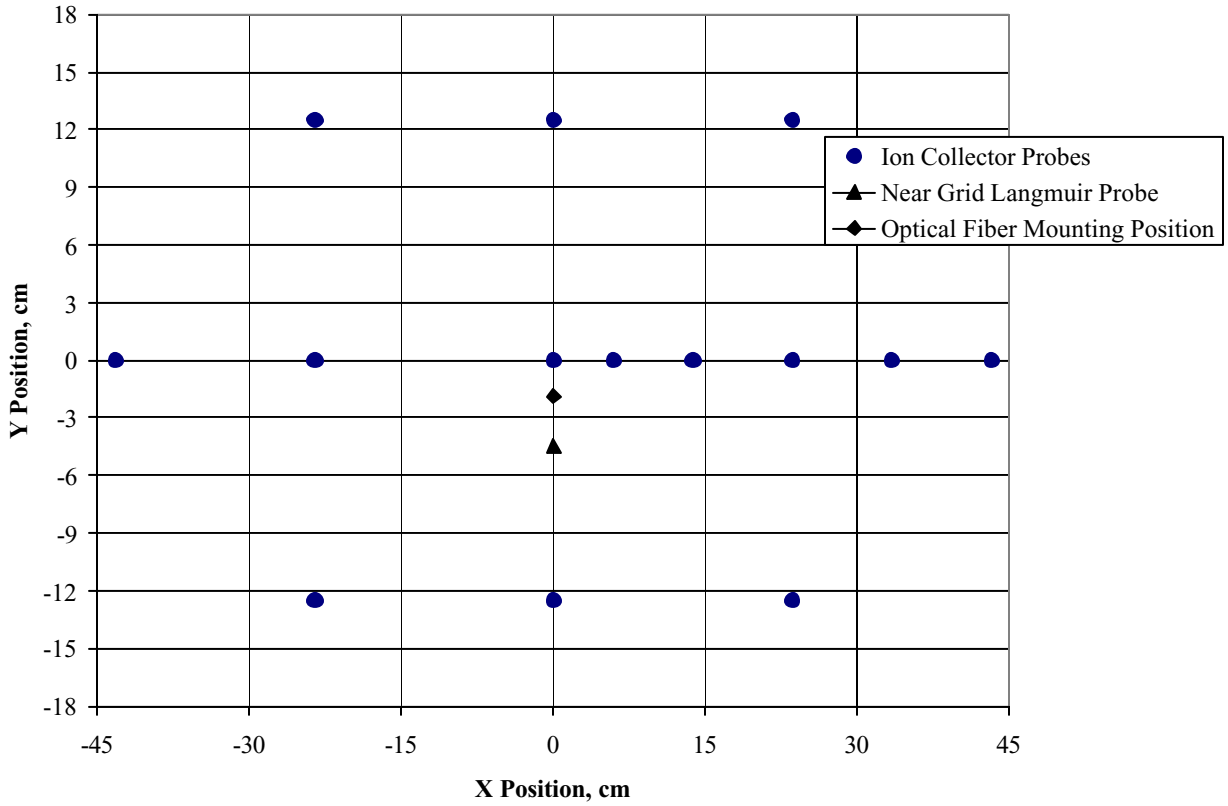

Figure 7. Locations of grid probe diagnostics. These include 14 planar grid probes, 1 single Langmuir probe and one centrally located optical fiber. (Note aspect ratio is not to scale)

In addition to the grid ion probes, a Langmuir probe was used to measure plasma properties local to the ion grid. The Langmuir probe, whose tungsten tip was 6 mm long and 0.21 mm in diameter, was located such that the middle of its active area was 2.3 cm upstream of the grid. The probe was located approximately 4 cm below the center of the grid. A second Langmuir probe was also used. This probe was located approximately 1 cm from the center of the backwall of the discharge chamber. In this respect, it sampled plasma produced near the microwave injection ports. A lens coupled to an optical fiber located approximately 4 cm above the center of the optics was used to collect light generated by the discharge plasma. The light was channeled to a monchromator with a 1 nm resolution. The purpose of the diagnostic was to provide a general survey of plasma species type and charge state.

Experimental Results: 5.85 GHz operation

The suitability of the microwave ECR discharge for high power ion thruster applications was assessed using a series of experiments and tests. These investigations were aimed at answering the following questions: 1) What is the thermal condition of the magnets at high power operation? 2) What is the sensitivity of matching to power and flow rate changes? 3) What is the uniformity of the discharge plasma? 4) What is the magnitude of the ion current available for extraction? 5) How does the plasma potential vary with operating condition? 6) What is the charge state distribution in the discharge? Experimental summaries addressing these questions may be found in the sub-sections that follow.

A. Assessment of magnet temperature during high power discharge operation

Because permanent magnets are used to establish the ECR excitation sites, characterization of the thermal state of the magnets during operation particularly at high power is important. The main objective of such a characterization exercise is to determine if the magnets during operation of the source reach temperatures such that irreversible changes in the residual magnetization occur. Because permanent magnets are necessary for plasma production and containment, magnet temperature variations with thruster power level must be documented for any thruster.[26] Degradation in magnetic field intensity can occur if the magnet operates above the thermal stabilization temperature. In the case of the rare earth magnets used here, the thermal stabilization temperature is 400 C. The goal of the optimizing the discharge chamber was to assure at least a 50 degree margin in magnet operating temperature so that the maximum operating temperature never exceeds 350 C. The magnetic field produced by these rare earth magnets degrades considerably once this temperature is exceeded and do not recover when the magnets are allowed to return to room temperature. The degradation occurs above this temperature because thermal agitation can permanently disrupt the alignment of the magnetic moments thereby destroying the bulk magnetization. Upon this occurrence, plasma containment and overall discharge performance also degrades leading to a possible failure in conditions necessary to sustain the discharge

In the past, particularly with DC devices, documentation of magnet temperature has been achieved using simple thermocouples.[26] It however is well known that thermocouple are susceptible to microwave radiation due to antenna effects which can lead to unreliable results.[27,28] In order to determine an upper limit or bound on the operating temperatures of the magnets in the microwave discharge, thermal paints were used instead of thermocouples. Such heat sensitive paints has seen widespread application particularly in rocket and gas turbine research. At a particular temperature, the paints will change color. Because the color change is irreversible, it serves as a post-test record of the maximum temperature reached.[29] To be effective, a series of different paints are typically used at each location of interest so that a temperature range of operation can be ascertained. In this investigation, three thermal paints were used: 1) 155 C, 2)275 C, and 3) 367 C. In this respect, the use of this triad provides a temperature range between 155 and 367 C. These colors were place on the magnet strips near the microwave applicators, as well as on the waveguide attached to the engine itself.

Analysis of the thermal paints post test revealed a number of interesting findings. For these tests, the discharge was operated at input microwave powers as high as 1700 W. Discharge tests were typically run from 1 to several hours of steady state operation. Post test analysis of the waveguide affixed to the engine revealed no change in the thermal paint color indicating that this structure did not reach 155 C. Analysis of the paint at the magnets suggested that the magnets also did not exceed 155 C as indicated by the presence of the unchanged paint. It should be pointed out that in certain regions where the paint was laid on rather thickly, the paint did spall. Also there was some evidence of carbonization at these sites; therefore, thick layers in this environment are to be avoided. All in all, however, the absence of a paint color change indicated that the magnets did not operate near the 350 C limit. Additionally, post test checkout of the surface magnetic field strength with a Gaussmeter confirmed these findings, indicating that within experimental uncertainties in the measurement, no change in magnetic fields strength had occurred.

D. Impedance matching

In general, a fraction of input microwave power can be expected to be reflected back to the microwave source because the nature of the load, the plasma, whose response is typically non-linear with variations in input power. This nonlinear nature is attributed to the fact that impedance changes can be affected by changes in the mode of absorption, changes to where the absorption takes place, and changes in plasma density near the microwave applicator just to name a few. Design considerations for microwave ion sources for ion thruster applications require

that this returned power fraction is manageable. This is particularly important for high power microwave discharges. Reflected power is be dealt with using radiators connected to loads at the circulator. Minimizing the reflected power minimizes the mass required both for the circulator, the dummy load and the radiator. In this investigation, the variation in the return loss was documented during discharge operation for all operating conditions. The return loss is a measure of the impedance mismatch. The return loss is defined as:[30]

$$\text{Return Loss (dB)} = 10*\text{LOG}_{10}(\text{Reflected Power/Incident Power}) \quad (6)$$

As can be seen from the experimental set up picture in Figure 6 the reflected and forward power were measured at a location downstream of the circulator. This arrangement allows the reflected power to be measured before it is absorbed at the circulator dummy load. The return loss ratio, which is a measure of the reflection coefficient, is plotted in Figure 9 for a number of operating conditions. As shown in the figure, the reflected power fractions were small, most less than 10% as indicated by the dashed line at -10 dB. The low return losses is an indicator that most of the forward power is going into the plasma. As suggested in this figure, it should be pointed out that in general matching, was for the most part independent of input power level or flow rate, indicating a relatively predictable upper limit on returned power for the plasma load.

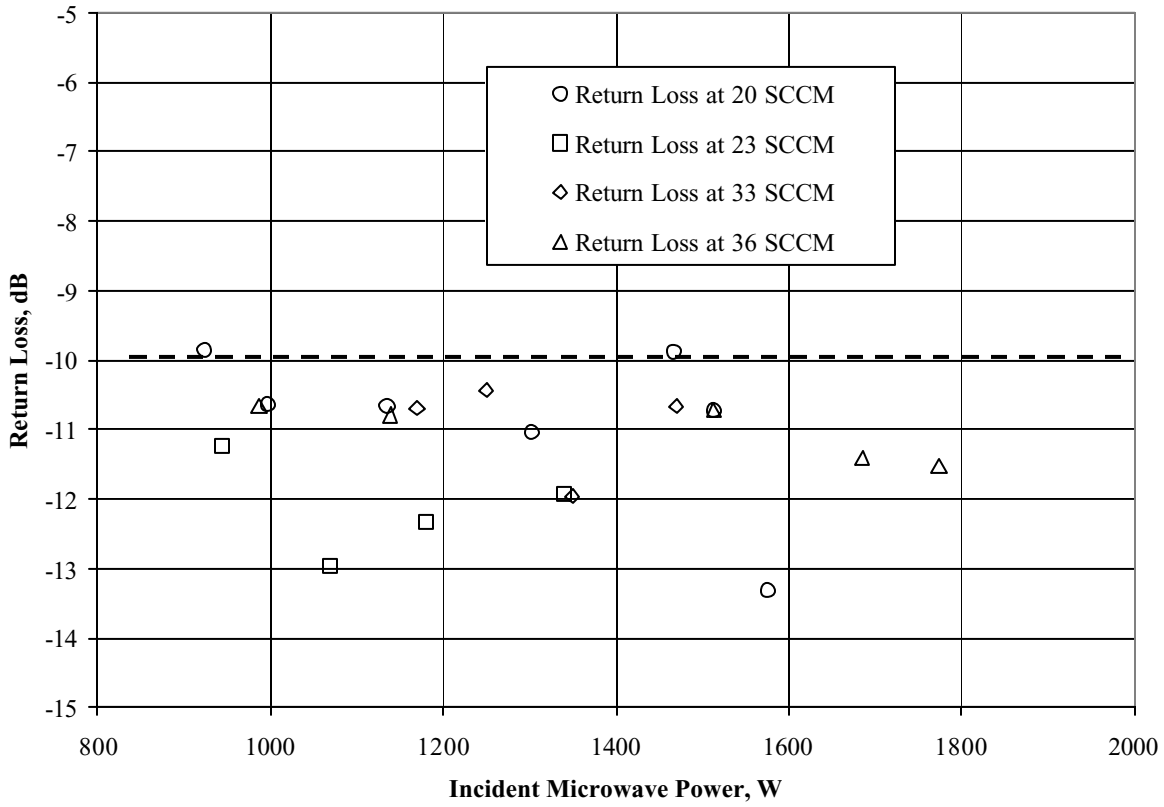

Figure 9. Variation in microwave return losses as a function of input power at different flow rates.

E. Plasma Uniformity and Average Extractable Ion Current

Plasma uniformity is an important discharge attribute. Non-uniformities in the plasma density profile can lead to crossover or direct impingement at locations where the plasma density is locally too low or too high respectively. These phenomena can limit the service life of the ion optics. High uniformity across the ion extraction plane assures that the electrostatic solution determined for the ion optics will yield a well-focused ion beam. The ion optics can be expected to wear uniformly in a predictable manner provided the plasma profile is uniform.

The geometry of the rectangular waveguide slotted antenna was well suited for integration into a rectangular discharge chamber. With these two components integrated together, the distributed plasma production capacity of the slotted antenna would be fully exploited to yield very uniform discharge plasmas. Consistent with this reasoning were observed plume profiles acquired during the 2.45 GHz beam extraction testing which had flatness parameters in excess of 80 percent. To test for uniformity at 5.85 GHz, wall probes were also utilized. The probes as indicated in Figure 7 were positioned to investigate uniformity along centerline as well as determine transverse uniformity and symmetry. Representative data taken at 20 SCCM is presented in Figure 10. Figure 10 illustrates the degree of lateral uniformity in the microwave discharge at the exit plane at 20 SCCM of xenon flow at 830 W and 1320 W of net microwave power. The points illustrated were laterally located along the middle of the discharge chamber extending from the geometric center to approximately 44 cm. The high density of probes along one side of the discharge chamber as illustrated in Figure 7 was used to assess the degree of uniformity in one half plane. To check for lateral symmetry, grid ion probe measurements were also made along the lateral center within the other half plane. These are labeled "lateral symmetry" in the Figure. As can be seen from the plot, within the uncertainty of the measurement, 5% in this case, the lateral symmetry points fall onto the profile, indicating very good lateral symmetry. This attribute of lateral symmetry is expected with the slotted antenna/rectangular discharge geometry. It should be pointed out that on centerline there is a slight dip in current density. This slight dip is attributed to the nature of plasma production at the microwave applicator, which is symmetrically displaced from the center by roughly a few centimeters.

A flatness or profile uniformity can be estimated for the span along the lateral center of the discharge chamber based on the ion probe data. In this case the lateral centerline profile flatness or uniformity can be defined as the ratio of the average current density along the centerline to the peak current density measured along the center. *At 20 SCCM, the discharge flatness was 0.92.* The plasma profile at 1320 W was similar to that of the 830 W case. For example, the shape of the profile as well as the presence small dip in current density near centerline was very similar. The discharge was also symmetrical along the centerline at the higher power. The discharge uniformity was also roughly equal at approximately *0.92*. Again, the high degree of flatness is a consequence of the distributed plasmas production associated with the slotted antenna.

In addition to lateral symmetry along the centerline, a truly uniform rectangular discharge must also demonstrate both lateral symmetry at off-centerline locations as well as top-to-bottom transverse symmetry. A survey of such lateral and transverse symmetry was achieved by acquiring ion current density measurements at off-center locations as a function of lateral position. To determine the degree of transverse symmetry and uniformity, probes were located 12.5 cm above or below the lateral centerline. Nine locations in all were compared. In this regard, this data is indicative of ion current density over a transverse distance of 25 cm and off axis lateral symmetry over nearly 50 cm. These comparisons are plotted in Figure 11 for the representative 20 SCCM case for two input microwave powers: 830 W and 1300 W. As can be seen in this Figure, not only is the ion current density relatively constant laterally at the off-axis position, but it is also relative constant in the transverse direction as well. This is illustrated by the bunching of the value of the ion current density at the centerline, the +12.5 cm and the -12.5 cm sampling positions. This holds true at both microwave powers. This data suggests a relatively flat, uniform plasma density profile over the entire extraction plane. Indeed, the average flatness parameter over this 25 cm transverse span for all locations was approximately 0.98 at both powers. Similar behavior was observed at higher flow rates as well. Small asymmetries between the top and bottom lateral profiles is attributed largely to slight misalignment of the ion grid whose center was located approximately 6 mm lower than the centerline of the discharge.

The relative flatness and high degree of lateral and transverse symmetry of the discharge allows for the estimation of the available extractable ion current at the exit plane from the ion probe measurements. An estimate of the available extractable ion current can be obtained by integrating over ion current profile measured across the lateral centerline. This region consists of the full lateral length of the discharge with the vertical integration limits extending 12.5 cm above and blow centerline. This region constitutes roughly 63 percent of the active area. Because it is expected that the plasma density should drop off at the edges, integrating over this sampled region should yield a good estimate of the lower limit of extractable ion current. The centerline current density profile is used in this way to calculate the ion current with the following relation:

$$I_{est} = \iint J(x,y)dxdy$$

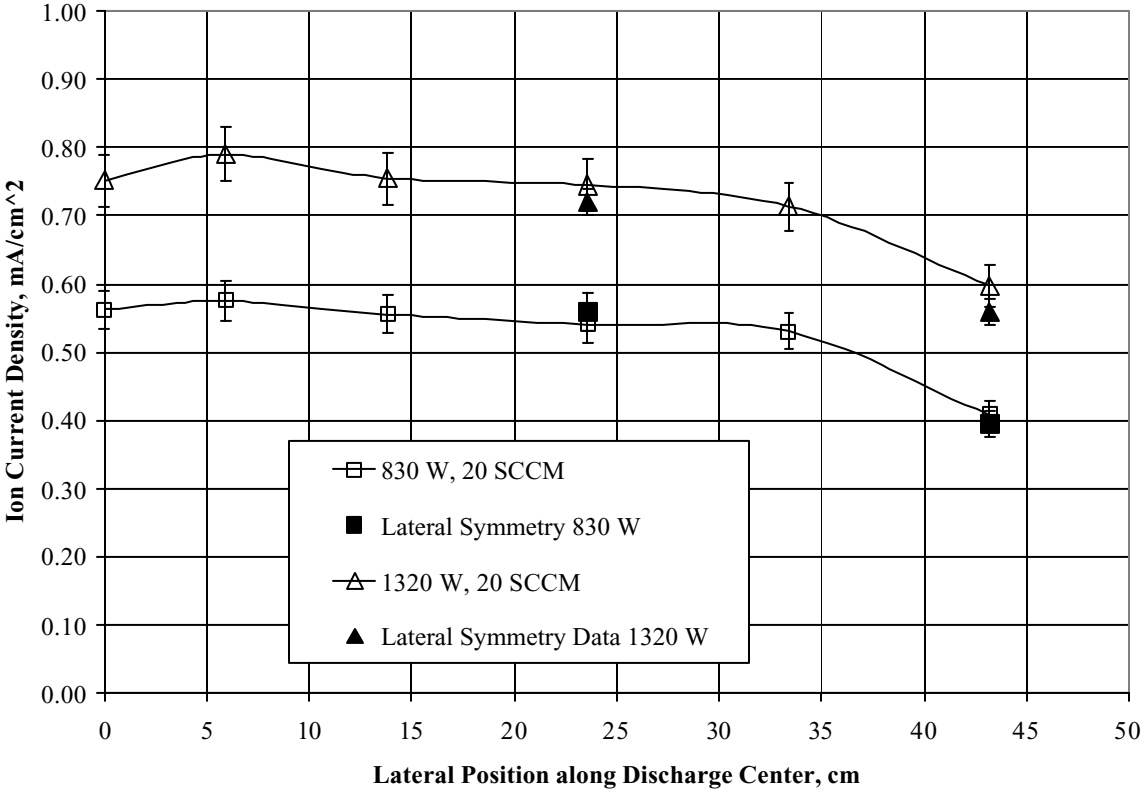

Figure 10. Variation in ion current density as acquired laterally along the center of the discharge as measured using planar probes within a half-plane. Lateral symmetry points taken at opposing sides (half-planes) of the discharge were used to demonstrate mirror/reflection symmetry.

Here, J(x,y) is a polynomial fit for the ion current density profile acquired on centerline using the button probes. The x limits range from -45 to 45 cm while the y limits range from -12.5 to +12.5 cm. Results of the integration for the 20 SCCM data and also representative data at 36 SCCM is presented in Table 1. Also shown in Table 1 is the Ampere equivalent for the associated flow rates.

Table I.

Xenon Flow Rate, SCCM	Net Microwave Power, W	Integrated Current Lower Limit, A	Ampere Equivalent
20	830	1.20	1.46
20	1320	1.64	1.46
35	900	1.43	2.62
35	1560	3.17	2.62

As can be seen in the table, the estimated ion current is an appreciable fraction of the maximum ion current extractable as defined by the Ampere equivalent at the respective flow rates. For the low flow rate condition, at 830 W, the estimated current is nearly 82% of the Ampere equivalent which is higher than the expected 63% based on integration area alone. At 1320 W, the estimated current is approximately 10 percent higher than the Ampere equivalent. Similar behavior is observed at the higher flow rate as well. The data appears to suggest that at higher powers, utilization is very high. Under these conditions, ingestion effects caused by the re-entry into the discharge by ions neutralized at the grid give rise to higher effective xenon flow rate. This process allows the actual ion current as measured on the grid to be higher than that then equivalent Ampere current. This phenomenon has been explained and can be accounted for by correcting for the ingested neutrals.[31]

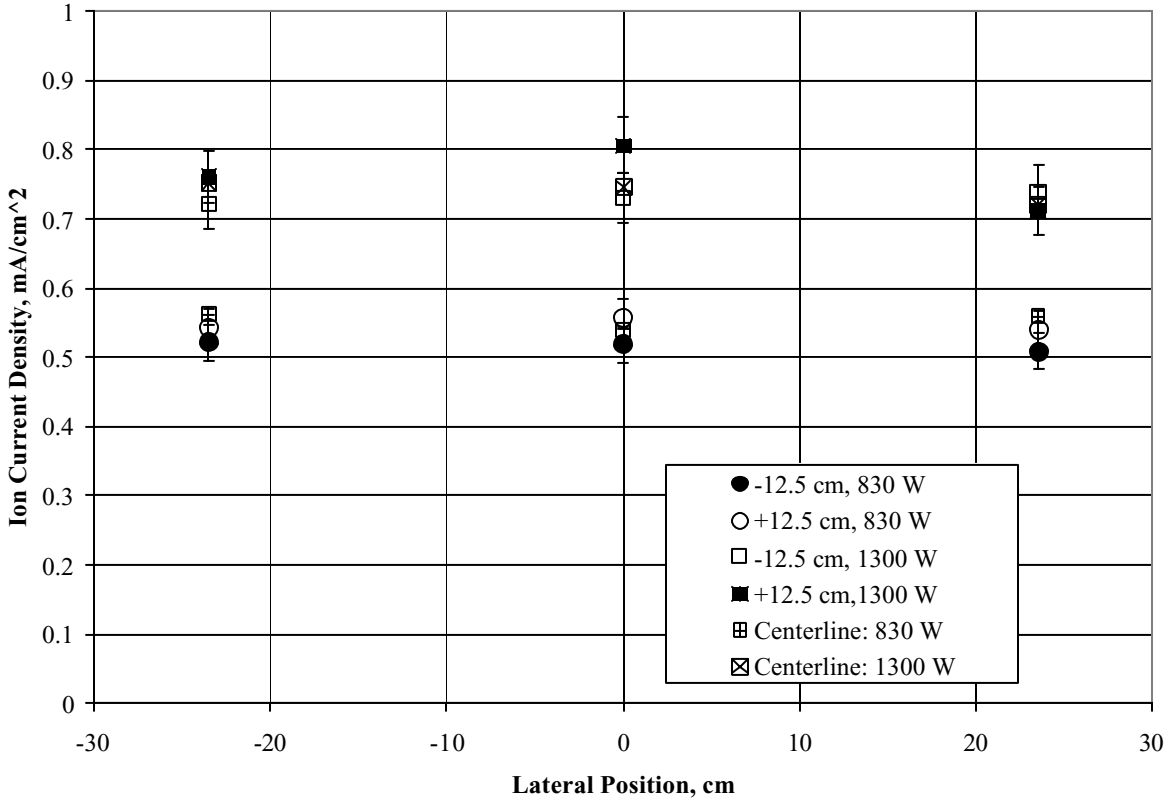

Figure 11. Transverse symmetry as assessed from off axis ion current density probes.

F. Langmuir Probe Measurements

A single Langmuir probe was used to measure plasma properties near the ion collector grid. The majority of the Langmuir probe surveys acquired were taken on centerline, approximately 2.3 cm upstream of the ion collector grid. Analysis of the Langmuir probe trace yields plasma potential, plasma number density, and electron temperature. The plasma potential provides insight into thruster lifetime, more specifically the lifetime of the screen grid electrode. Ions falling out of the discharge impact the screen grid electrode. If their energies are in excess of the sputtering threshold then erosion will take place. The plasma potential measured near the screen grid can be used to estimate this energy. The nature of the potential difference between the screen and the plasma also effects beamlet divergence. For a given total extraction voltage for a perfectly aligned set of ion optics, the smaller the potential difference between the screen and plasma, the lower the beamlet divergence. Ion density is also of interest in that it is a direct measure of the coupling efficiency of microwaves to the plasma as well as a measure of how close the source is operating to cut-off densities. Additionally, it provides insight into plasma "choking" effects at the applicator due to local high density operation. The electron temperature provides insight into the nature of ionization processes, microwave coupling efficiency as well as plasma loss rates at the walls.

1. Plasma potential

Figure 12a illustrates the behavior of plasma potential variations with net input microwave power. As can be seen from the figure at a given flow rate, the plasma potential, within the uncertainty of the measurement, does not vary appreciably with microwave power at a given flow rate. The figure does indicate that the magnitude of the plasma potential is lower at the higher flow rate. The potential difference between the ion grid and the plasma potential can be taken to be equal to these measured plasma potentials. This sheath voltage, comparatively speaking ranges between 10 to 15 V lower than that observed in DC ion thrusters, where this potential difference is approximately equal to the discharge voltage, ~26 V. This plasma potential comparison shows a potential benefit of

microwave plasma sources. The lower associated plasma potentials correspond to reduced erosion rates at the screen grid and therefore improved screen grid lifetime.

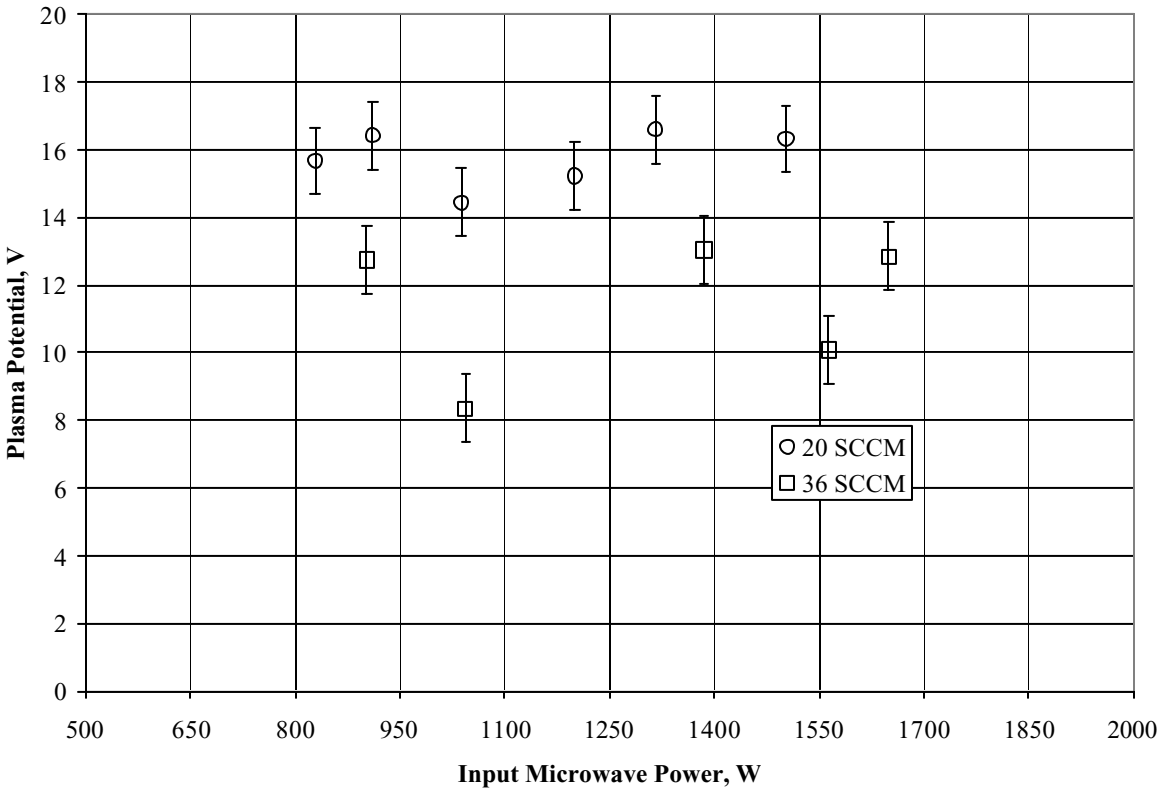

Figure 12a. Variation in plasma potential with increasing microwave power.

2. Plasma density

Figure 12b depicts the variation in the near ion grid plasma density with increasing microwave power at two flow rates. As can be seen here, at a given input power, the plasma density is higher at the higher flow rate. At the lower flow rate the data indicates a monotonic increase in plasma density up to approximately 1200 W. Beyond 1200 W, the plasma density appears to saturate, increasing at a much reduced rate with increasing input power. Saturation in the density occurs either because the plasma density at the applicator has reached its cut-off value or that utilization is sufficiently high so increasing density requires increasingly higher microwave input powers. The high calculated grid currents suggest that the latter possibility likely prevails. At the higher xenon flow rate, 36 SCCM, there is an initial abrupt rise in density with power leading to a power range over which the density increases only slightly with increasing power. Interestingly enough, beyond 1500 W of input, the rate of density increase with power takes off once again. This rise at the higher powers suggests improved ionization which could be due to tunneling phenomena at the applicator or resonant plasma production taking place at other regions in the discharge chamber where the magnetic field is sufficiently high for ECR to take place. This latter possibility can occur once the microwave intensity at a distant magnet ring is sufficiently high to drive ionization processes there. Such transitions have been observed to occur with increasing microwave input power.[16]

Figure 12c illustrates the behavior of the plasma density as a function of input xenon flow rate at a fixed input power. As expected, the plasma density is larger at a given flow rate as power is increased. For both powers shown here, there is a local maximum in the plasma density as a function of flow rate. This local maximum suggests that at a given power, there is an optimum operating flow rate. It was observed at this optimum points, the plasma potential and electron temperature were low (~10 V, 1.4 to 1.7 eV). At this condition, the ion production cost is minimized. At fixed input power, one would expect the density to rise monotonically with flow rate. The decrease in density at

the higher flow rates is likely due to electron temperature cooling. The peak in density shifts to the right toward higher flow rates with increasing microwave power. This is also expected. The plasma production rate is proportional to power and flow rate. Competition between electron cooling and the plasma production rates should give rise to the measured shift observed in Figure 12c.

Plasma density measurements were also made near the ECR zones of the slotted antenna. Plasma density measurements made here indicated over an order of magnitude higher plasma densities than those measured at the ion grid. The measurements here however tended to be very noisy. Detailed interrogation of these regions will require more sophisticated diagnostic techniques as the static magnetic field and time varying electric field are high there. This investigation is left to future work.

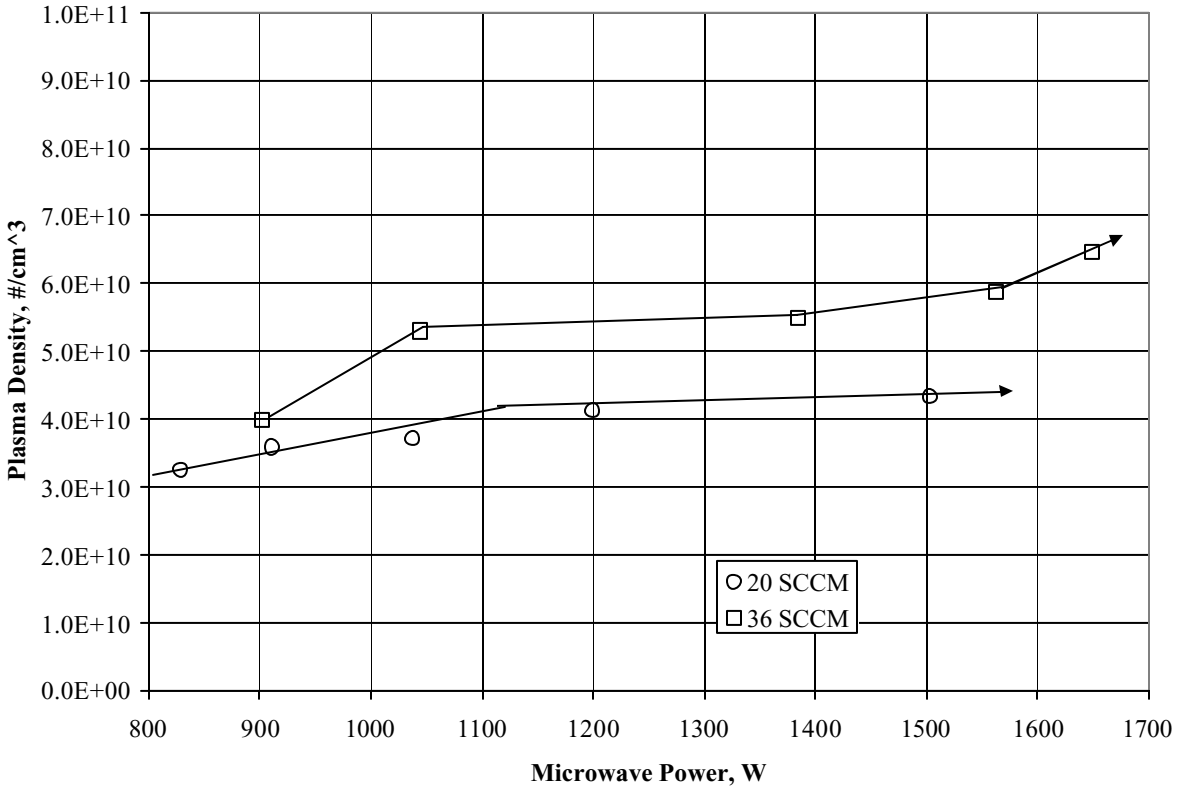

Figure 12b. Plasma density variations with input microwave power.

3. Electron Temperature

The electron temperature near the grid did not exhibit an definite trend with increasing microwave power. The electron temperature was lower at the higher flow rate. This observation is consistent with collisional cooling. Over the power range investigated, at 20 SCCM, the electron temperature varied around 2.5 eV(delta ~0.5 eV). At 36 SCCM the electron temperature tended to vary about 2 eV with the same delta of about 0.5 eV. The insensitivity of the electron temperature to increasing power is a behavior that is similar to that observed in electropositive DC discharges.[32] Apparently, over the power range investigated here, electron temperature is not a monatonically increasing function of power. This behavior seems to suggest that the power is going into plasma production rather than heating the electrons. This is consistent with a very hot electron population confined to the ECR zones distant from the ion grid. A more detailed analysis of the distribution function would be required to validate this assertion. Such an investigation is left to future work.

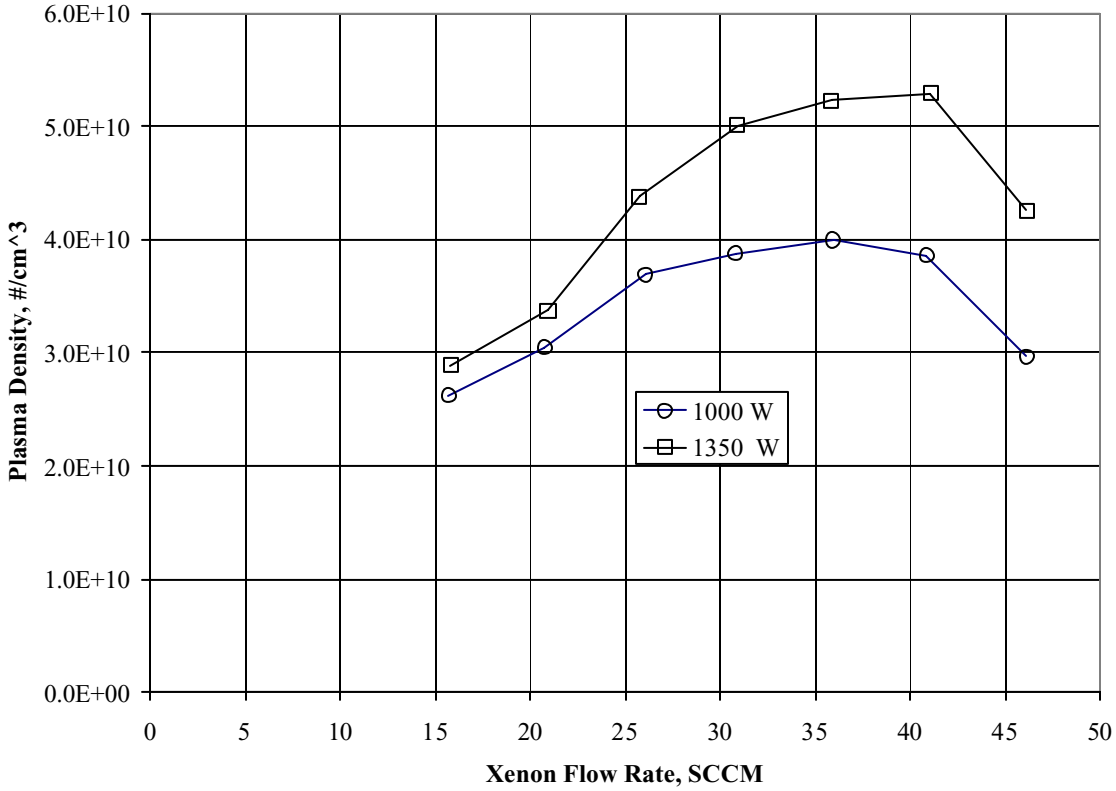

Figure 12c. Variation in plasma density with increasing flow rate.

G. Emission Spectra

In addition to plasma measurements, emission spectra were acquired at various operating conditions. The optical fiber and lens unit acquired emission from the central regions of the discharge chamber. The purpose of acquiring the spectra was to assess the species present in the discharge plasma as well as determine qualitative plasma changes with input microwave power. The spectra were dominated by xenon lines with no detectable presence of impurities. As ascertained from the xenon spectra, doubly-charged xenon lines were absent. Figure 14 depicts representative spectra acquired at 36 SCCM and 1650 W. As shown here, the discharge spectra are dominated by singly charged xenon lines. These lines with the exception of the xenon neutral lines located around 823 nm were among the most intense observed. It is interesting to note that with increasing microwave powers there is spectral evidence of a decrease in the neutral population at least in the region interrogated. Figure 15 illustrates the variations in peak intensities for xenon ion lines and xenon neutral lines with input microwave power. Due to its relative closeness to the xenon neutral line at 483 nm, the 484 nm line was not plotted. As can be seen in the figure, on average, with the exception of the small dip around 1130 W, as a function of increasing microwave power, the xenon ion line peak intensities increased with increasing microwave power. Of interest is the relative insensitivity of the neutral lines to increasing microwave power. In some cases, the neutral lines actually decrease in peak intensity with increasing microwave power. Over this power range the plasma density increases monotonically while the electron temperature was observed to decrease somewhat. The decrease however was within the uncertainty of the measurement. The small decrease in the neutral line intensity and the associated monotonic increase in the ion intensity suggest simple conversion (local depletion) of neutrals to ion as the ionization fraction increases with increasing input power

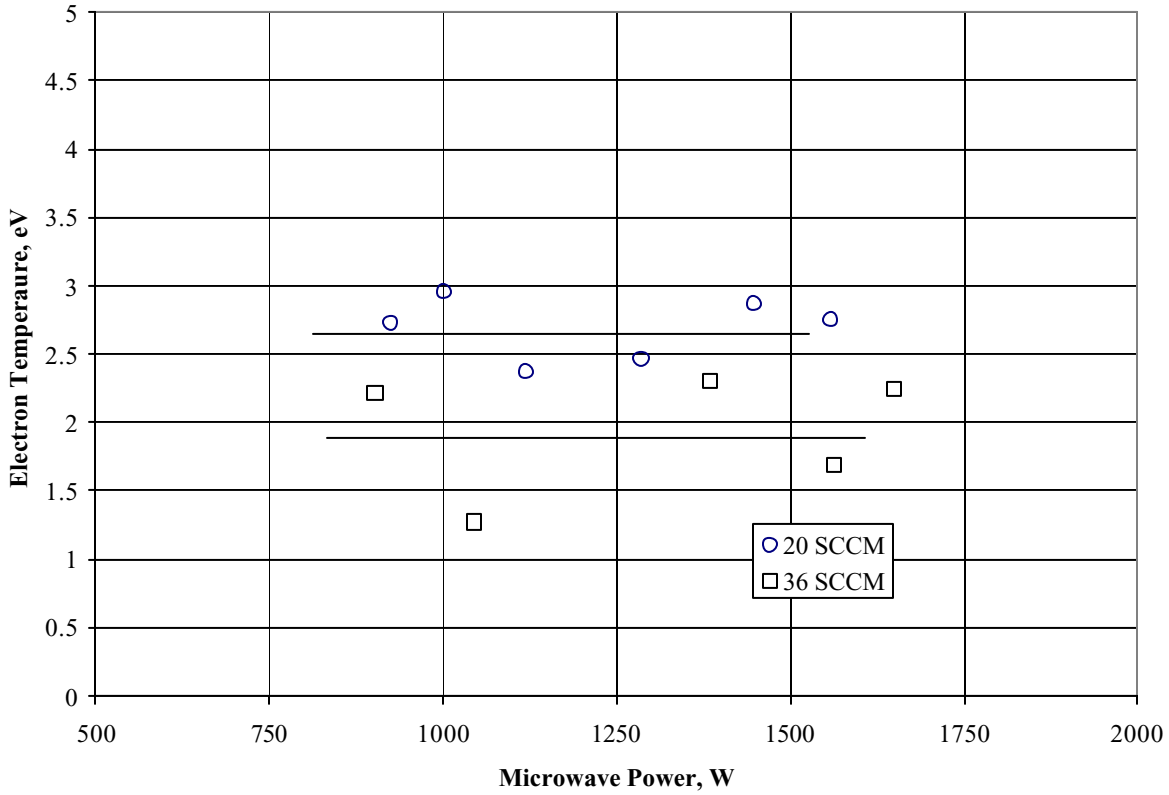

Figure 12d. Variation in electron temperature with increasing microwave power.

Conclusions

Microwave based ion thrusters offer potential lifetime advantages over conventional DC ion thrusters. For aggressive missions requiring long thrusting times (~10 years), the microwave technology can potentially satisfy discharge lifetime requirements, leaving the ion optics as the main ion thruster failure mode. With the incorporation of carbon based grids, even this failure mode can be all but eliminated. In this regard, microwave-based ion technology potentially has a bright future particularly for high power missions to the outer planets and beyond. As with any emerging technology, further development will be required to realize the benefits of this approach. Such development should focus primarily of the development of a full scale microwave thruster system including microwave neutralizer technology and power processing unit. The work presented herein focused on documenting the operating characteristics of one aspect of such a system, the discharge. Discharge chamber operating temperature range, as determined using thermal paints, was found to be well below the magnet's thermal limit 350 C. Impedance matching measurements indicated that over the 500W to 2500 W power range, less than 5 percent of the power was reflected back. The discharge plasma proved to be very uniform both laterally and in the transverse direction. Lateral flatness parameters estimated along the lateral center of the discharge were calculated to be greater than 90%. Plasma potentials were (in many cases of order 10 V) well below that typical of DC thrusters. At a fixed microwave power, as the flow rate was varied, a maximum in performance as indicated by a peak in the plasma density was found. Electron temperature was found to be relatively insensitive to changes in microwave power. Emission spectra revealed the plasma to be dominated by xenon lines with no sign of impurities or doubly charged xenon.

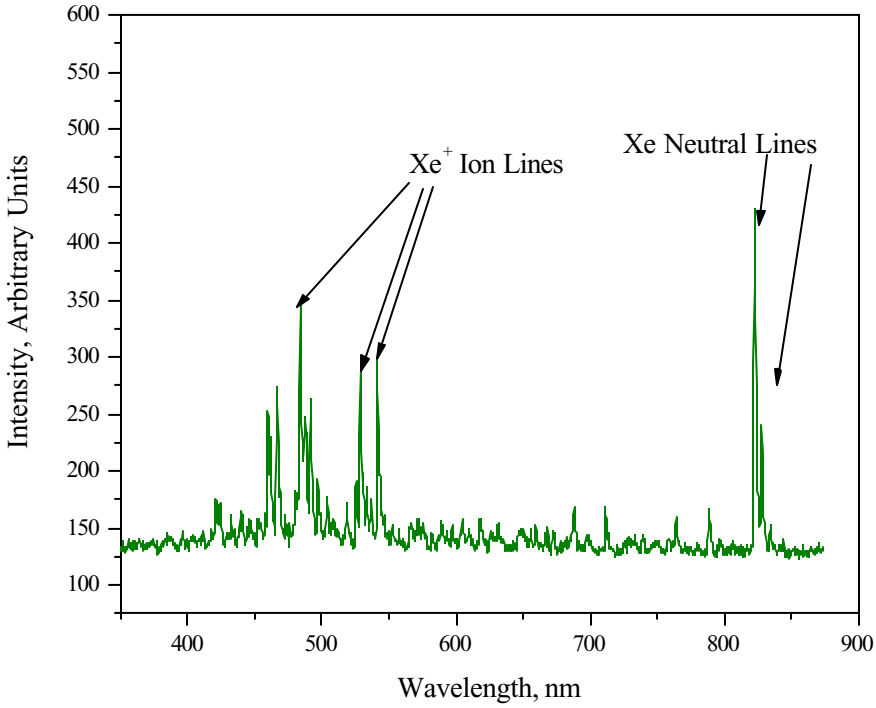

Figure 13. Representative emission spectra acquired at 36 SCCM and 1650 W microwave power.

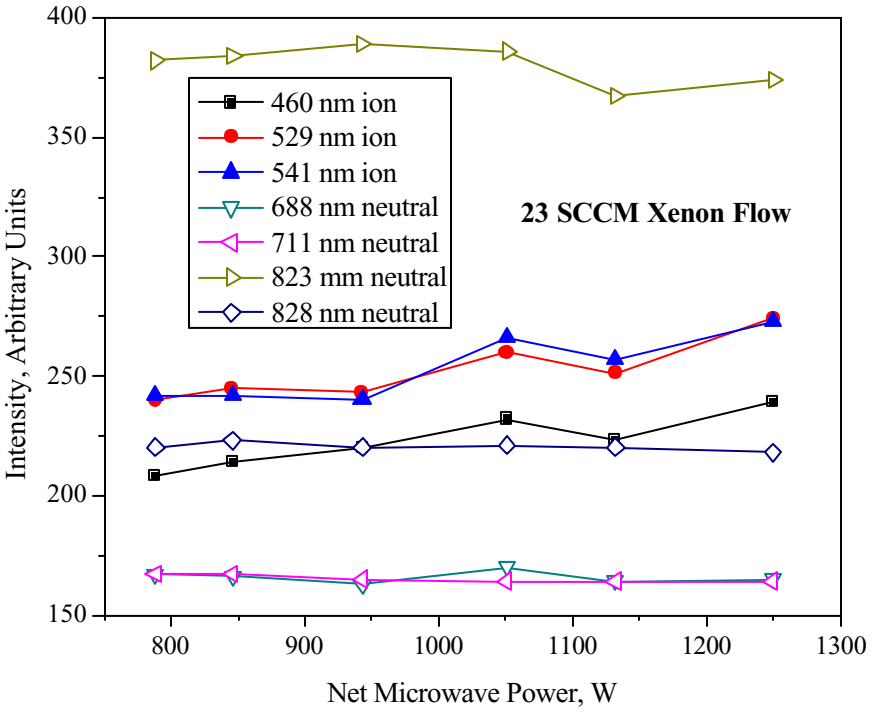

Figure 14. Variation in representative ion and neutral line peak intensities with input microwave power.

References

[1]Foster, J.E. et al, "The HiPEP Thruster," Proceedings of the 40th Joint Propulsion Conference, AIAA Paper 2004-3812, July 2004.

[2]Oleson, S., "Electric Propulsion Technology Development for the Jupiter Icy Moon Orbiter Project," Proceedings of the 40th Joint Propulsion Conference, AIAA Paper 2004-3449, July 2004.

[3]Williams, G.W. , Sovey, J., and Haag, T., "Performance Characterization of HiPEP Ion Optics," AIAA Paper 2004-3627, July 2004.

[4]Sarver-Verhey, T.R., "Scenario for Hollow Cathode End –of-Life," 26th International Electric Propulsion Conference, Kitakyushu, Japan, October, 1999, NASA/CR 2000-209420.

[5]Patterson, M.J. et al, "Recent Development Activities in Hollow Cathode Technology," International Electric Propulsion Conference, Pasadena, October 2001, IEPC paper 01-270.

[6]Kovaleski, S.D. et al, "A review of Hollow Cathode Testing for the international Space Station Plasma contactor," IEPC Paper 01-271.

[7]Sengupta, A., Brophy, J. R., Goodfellow, K. D., "The Extended Life Test of the Deep Space 1 Flight Spare Ion Engine after 30,352 Hours of Operation," AIAA-2003-4558, presented at the 2003 Joint Propulsion Conference, Huntsville, AL, July 20-23, 2003.

[8]Rovey, Josh, and Gallimore, A.D., "Design and Operation of a Multiple Cathode, High Power, Rectangular Discharge Chamber," 41st AIAA/ASME/SAE/ASEE Joint Propulsion Conference, 10-13, July 2005, Tucson, AIAA paper 2005-4407.

[9]Vaughn, J.A. et al, "NEXIS Reservoir Cathode 2000 Hour Proof-of –Concept Test," 40st AIAA/ASME/SAE/ASEE Joint Propulsion Conference, July 2004, Fort Lauderdale, AIAA paper 2004-4203.

[10]Van Noord, J., Kamhawi, H., and Patterson, M.J., "High Current Hollow Cathode," 29th International Electric Propulsion Conference, Princton, IEPC Paper 2005-321.

[11]Bering, E.A., Chang-Diaz, F., and Squire, J., "The Use of RF Waves in Space Propulsion Systems," *The Radio Science Bulletin*, No. 310, Sept. 2004, pp. 92-106.

[12]Roth, R. Industrial Plasma Engineering: Volume I, Institute of Physics publishing, 2001

[13]Foster, J.E. and Patterson, M.J., "Microwave ECR Ion Thruster Development Activities at NASA GRC," 38th Joint Propulsion Conference, Indianapolis, July, 2002, AIAA Paper 2002-3837

[14]Divergilio, W.F. et al, "High Frequency Plasma Generators for Ion Thrusters," NASA CR-167957, November, 1981.

[15]Kuninaka, H., "Flight Report During Two Years on Hayabusa Explorer Propelled by Microwave Discharge Ion Engines," 41st Joint Propulsion Conference, Tucson, July 10-13, 2005, AIAA Paper 2005-3673.

[16]Foster, J.E. and Patterson, M.J., "Discharge characterization of 40 cm –microwave ecr ion source and neutralizer,"38th Joint Propulsion Conference, Huntsville, July 2003, AIAA 2003-5012.

[17]Kamhawi, H., Foster, J.E., and Patterson, M.J., "Operation of a microwave electron cyclotron resonance cathode," 40th Joint Propulsion Conference, Fort Lauderdale, July 11-14, 2004, AIAA Paper 2004-3819.

[18]Kamhawi, H., "High current ECR plasma cathode," 28th International Electric Propulsion Conference, Sacramento, IEPC paper 2005-2005.

[19]Hayakawa, Y., Miyazaki, K., and Kitamura, S., "Measurement of Electron Energy Distributions in a 14 cm Diameter Ring Cusp Ion Thruster," Joint Propulsion Conference, AIAA Paper 89-2715, July 1989.

[20]Foster, J.E., Soulas, G.C., and Patterson, M.J., "Plume and Discharge Plasma Measurements of an NSTAR-type Ion Thruster," 36th Joint Propulsion Conference, Huntsville, July 2000, AIAA Paper 2000-3812.

[21]Foster, J.E., Soulas, G.C., and Patterson, M.J>, "Plume and Discharge Plasma Measurements of an NSTAR-type Ion Thruster," 36th Joint Propulsion Conference, 16-19 July 2000, Alabama, AIAA Paper 2000-3812.

[22]Jasik, H., Editor, Antenna Engineering Handbook, McGraw Hill Book Company, New York, Chapter 9, 1961.

[23]Personal communication via presentation entitled " Ion Thruster Efficiency Sensitivity Analysis", Steve Oleson March 3, 2004.

[24] Patterson, M.J, et al, "Next-generation 5/10 kW Ion Propulsion Development Status," 27th International Electric Propulsion Conference, Pasadena, CA, 15-19 October 2001, IEPC Paper 01-089.

[25] Kuninaka, H., Satori, S., Funaki, I., Shimizu, Y., and Toki, K., "Endurance Test of Microwave Discharge Ion Thruster System for Asteroid Sample Return Mission MUSES-C," IEPC Paper 92-137, 26th IEPC, Cleveland, 1997.

[26] Sarver-Verhey, T.R, Domonkos, M.T., and Patterson, M.J., "Thermal characterization of a NASA 30 cm ion thruster operated up to 5 kW", 38th Joint Propulsion Conference, Huntsville July 2000, AIAA Paper 2000-3816.

[27]Chakraborty, D.P., and Brezovich, I.A., "Error sources affecting thermocouple thermometry in RF electromagnetic fields" Journal of Microwave Power, 17 (1), 1982, pp. 17-28.

[28]Pert, E. et al, "Temperature measurements during microwave processing: The significance of thermocouple effects," Journal of the American Ceramic Society, Vol 8 no. 9, pp 1981-1986, 2001.

[29]Childs, P.R.N, Greenwood, J.R. and Long, C.A.., "Review of temperature measurement," *Review of Scientific Instruments*, Vol. 71, No. 8, August 2000, pp. 2959-2978.

[30]Laverghetta, T. S., Practical Microwaves, Howard W. Sams and Company, Inc., Indianapolis, pp. 33-36, 1984.

[31]Brophy, J.R., "Simulated Ion Thruster Operation without Beam Extraction," AIAA, DGLR, and JSASS. 21st International Electric Propulsion Conference, Orlando, FL, 1990, AIAA Paper 90-2655.

[32]Lieberman, M and Lichtenberg,, A., Principles of Plasma Discharges and Materials Processing, Chapter 10, Wiley & Sons, NY, 1994.